NASA/TM–2018-220081

Undirectional Carbon Nanotube Yarn/Polymer Composites

Jae-Woo Kim
National Institute of Aerospace, Hampton, Virginia

Godfrey Sauti, Russell A. Wincheski, Roberto J. Cano, Benjamin D. Jensen, Joseph G. Smith Jr., Kristopher E. Wise, and Emilie J. Siochi
Langley Research Center, Hampton,Virginia

July 2018

NASA STI Program . . . in Profile

Since its founding, NASA has been dedicated to the advancement of aeronautics and space science. The NASA scientific and technical information (STI) program plays a key part in helping NASA maintain this important role.

The NASA STI program operates under the auspices of the Agency Chief Information Officer. It collects, organizes, provides for archiving, and disseminates NASA's STI. The NASA STI program provides access to the NTRS Registered and its public interface, the NASA Technical Reports Server, thus providing one of the largest collections of aeronautical and space science STI in the world. Results are published in both non-NASA channels and by NASA in the NASA STI Report Series, which includes the following report types:

- TECHNICAL PUBLICATION. Reports of completed research or a major significant phase of research that present the results of NASA Programs and include extensive data or theoretical analysis. Includes compilations of significant scientific and technical data and information deemed to be of continuing reference value. NASA counter-part of peer-reviewed formal professional papers but has less stringent limitations on manuscript length and extent of graphic presentations.

- TECHNICAL MEMORANDUM. Scientific and technical findings that are preliminary or of specialized interest, e.g., quick release reports, working papers, and bibliographies that contain minimal annotation. Does not contain extensive analysis.

- CONTRACTOR REPORT. Scientific and technical findings by NASA-sponsored contractors and grantees.

- CONFERENCE PUBLICATION. Collected papers from scientific and technical conferences, symposia, seminars, or other meetings sponsored or co-sponsored by NASA.

- SPECIAL PUBLICATION. Scientific, technical, or historical information from NASA programs, projects, and missions, often concerned with subjects having substantial public interest.

- TECHNICAL TRANSLATION. English-language translations of foreign scientific and technical material pertinent to NASA's mission.

Specialized services also include organizing and publishing research results, distributing specialized research announcements and feeds, providing information desk and personal search support, and enabling data exchange services.

For more information about the NASA STI program, see the following:

- Access the NASA STI program home page at http://www.sti.nasa.gov

- E-mail your question to help@sti.nasa.gov

- Phone the NASA STI Information Desk at 757-864-9658

- Write to:
  NASA STI Information Desk
  Mail Stop 148
  NASA Langley Research Center
  Hampton, VA 23681-2199

NASA/TM–2018-220081

Undirectional Carbon Nanotube Yarn/Polymer Composites

Jae-Woo Kim
National Institute of Aerospace, Hampton, Virginia

Godfrey Sauti, Russell A. Wincheski, Roberto J. Cano, Benjamin D. Jensen, Joseph G. Smith Jr., Kristopher E. Wise, and Emilie J. Siochi
Langley Research Center, Hampton,Virginia

National Aeronautics and
Space Administration

Langley Research Center
Hampton, Virginia 23681-2199

July2018

Acknowledgments

This work was funded through the NASA Space Technology Mission Directorate Program. The authors thank Mr. Hoa H. Luong, [NASA Langley Research Center (LaRC)] and Mr. Sean M. Britton (NASA LaRC) for their assistance with composite processing, Mr. John W. Hopkins (NASA LaRC) for laser cutting, Prof. Michael Czabaj (University of Utah) for conducting the short beam shear tests, and Prof. Richard Liang and Dr. Jin Gyu Park (Florida State University) for the TEM work.

Available from:

NASA STI Program / Mail Stop 148
NASA Langley Research Center
Hampton, VA 23681-2199
Fax: 757-864-6500

ABSTRACT

Carbon nanotubes (CNTs) are one-dimensional nanomaterials with outstanding electrical and thermal conductivities and mechanical properties at the nanoscale. With these superior physical properties, CNTs are very attractive materials for future light weight structural aerospace applications. Recent manufacturing advances have led to the availability of bulk formats of CNTs such as yarns, tapes, and sheets in commercial quantities, thus enabling the development of macro-scale composite processing methods for aerospace applications. The fabrication of unidirectional CNT yarn/polymer composites and the effect of processing parameters such as resin type, number of CNT yarn layers, CNT yarn/resin ratio, consolidation method, and tension applied during CNT yarn winding on the mechanical properties of unidirectional CNT yarn composites are reported herein. Structural morphologies, electrical and thermal conductivities, and mechanical performance of unidirectional CNT yarn/polymer composites under tensile and short beam shear loads are presented and discussed. The application of higher tension during the winding process and elevated cure pressure during the press molding step afforded a compact structural morphology and reduced void content in the composite. However, the composite tensile strength was negligibly impacted by the fabrication parameters, such as cure pressure, winding tension, and resin chemistry, excepting resin content and number of CNT yarn layers. The tension winding method produced better quality and lower resin content CNT yarn composites compared to conventional prepregging methods, resulting in higher specific strength and modulus of the composites. The specific tensile strength of the CNT composite was approximately 69 % of the starting CNT yarn. Electrical and thermal conductivities of unidirectional CNT yarn/polymer composites were in the range of 1000 to 12000 S/cm and 22 to 45 W/m·K, respectively.

Introduction

Carbon nanotubes (CNTs) have been widely studied for various aerospace applications due to their excellent combination of electrical, thermal, and mechanical properties. These applications include high current carrying capacity wires,[1-2] electromagnetic interference shielding,[3] thermal protection,[4] and structural components.[5] A particular focus has been placed on lightweight structural applications because individual CNTs exhibit superior elastic tensile moduli (~ 1 TPa) and breaking strengths (~100 GPa) on the nanoscale.[6-9] However, the promising mechanical properties of individual CNTs have not translated to lightly doping (< 20 wt.% of CNTs in polymer matrix) macroscale CNT composites due to poor load transfer both between the CNTs or CNT bundles and between the CNTs and polymer matrix.[10-14]

Windle et al. reported tensile and compressive mechanical properties of aligned CNT fibers with 10-30 vol.% in an epoxy matrix.[15] The low density of the CNT fibers (0.55 g/cm^3) enabled epoxy infiltration, which can reduce compressive buckling of the nanotube bundles within the fibers. The specific tensile strength of the 27 vol.% composite was 230 MPa/(g/cm^3) and the specific yield stress of the 14 vol.% composite in compression was 118 MPa/(g/cm^3). The ultimate tensile strength of the CNT fiber/epoxy composite studied was found to be 90 % of the value predicted by the simple rule of mixtures with some assumptions. While these results represent large increases over the pure epoxy, which has a specific tensile strength of 35.8 MPa/(g/cm^3) and a specific yield stress of 33.3 MPa/(g/cm^3), they are substantially lower than the nanoscale properties of the CNT constituent. Further improvement in composite properties will require better as-spun fiber properties than the 1.0 GPa/(g/cm^3) tensile strength and 40 GPa/(g/cm^3) tensile stiffness fibers used in that study, as well as higher fiber volume fractions in the composites.

Recent developments in CNT manufacturing have led to the availability of large quantities of CNT assemblages, such as yarns, tapes, and sheets, with consistent mechanical properties.

Although this progress in manufacturing and advances in CNT composite processing techniques have renewed interest in the potential for high strength structural CNT composites,[16-24] these improvements were achieved on the scale of individual CNT yarns and sheets. Realizing high performance and light weight structural composites will require the fabrication of composites with multiple layers of CNT sheets or CNT yarns to determine if the materials can truly compete with state-of-the-art carbon fiber (CF) composites in properties needed for the broad aerospace applications envisioned for this material.

In this work, the fabrication of unidirectional CNT yarn/polymer composites with CNT mass fractions exceeding 70 wt.% was demonstrated and the influence of the processing conditions on the structural morphologies and mechanical properties was evaluated. Typical CF composite processing parameters were considered for the fabrication of CNT composites to evaluate their transferability between material systems. The tensile properties of the CNT composites are discussed along with their dependence on various resin types, winding tensions, number of CNT yarn layers, and resin cure methods and pressures.

Experimental Section

Matrix. Three thermosets were used as polymer matrices for this study. EPON™ 828, API-60, and cyanate ester (RS-16) were obtained from Hexion Inc., Applied Poleramic Inc., and Tencate Advanced Composites, respectively. EPON™ 828 is a two-part difunctional bisphenol A/epichlorohydrin derived liquid epoxy resin with a fully cured resin density of 1.16 g/cm^3. EPIKURE™ W was used as the cure agent. API-60 is a toughened epoxy system having a high modulus retention at elevated temperature (over 2 GPa at 200 ^{o}C). The glass transition temperature (T_g) is 206 ^{o}C when cured using a standard 177 ^{o}C cure cycle. The cyanate ester resin is a low temperature, low viscosity two-part resin system with an excellent pot life (230 min at 75 ^{o}C or 60

min at 100 °C). The resin density and T_g are 1.21 g/cm^3 and 149.4 °C, respectively, without post cure.

Materials and composite processing. As-received highly-densified CNT yarns (Nanocomp Technologies, Inc.) were used to prepare unidirectional CNT yarn/polymer composites. The CNT yarns were composed of either 1, 2, or 4-plies of CNT roving with minimal physical twisting. For composite processing, EPON™ 828 and API-60 were diluted with methyl ethyl ketone (MEK, Sigma-Aldrich) to yield 70 wt.% and 50 wt.% resin concentrations, respectively. In the case of the cyanate ester, a 65 wt.% MEK solution of resin (Part A) was mixed with 65 wt.% MEK solution of curing agent (Part B). The mix ratios between Part A and Part B were 100 to 25 for EPON™ 828 and 100 to 9 for the cyanate ester. The resin solutions were applied directly onto the CNT yarns by a wet winding method using a custom-built filament winder.[5] The process involved passing CNT yarn through a resin bath followed by direct winding onto custom-made fixtures including an adjustable stainless-steel rod fixture (width of 30.48 cm and rod spacing of either 15.24 or 30.48 cm) and solid aluminum plates (width of 15.24 cm and height of either 6.35 or 10.16 cm), as shown in Figure 1. Winding tensions applied to the CNT yarn were varied between 2.49 and 13.34 N to explore their impact on composite morphology and mechanical properties. For samples prepared on the stainless-steel rod fixture, the as-wound unidirectional CNT yarn/polymer composites were placed in a custom-made press mold equipped with a pair of corrugated bars to hold the sample under tension during the cure process. In this fixture, additional tension was applied to the wound CNT yarns during the clamping process. For samples prepared on the solid aluminum plate fixtures, the as-wound CNT yarn/polymer composites were sandwiched between two steel plates and cured under the desired pressure and temperature. The CNT yarn/EPON™ 828 and CNT yarn/API-60 materials were cured with a 1 hr hold at 100 °C followed by a 2 hr hold at 177 °C. Unidirectional CNT yarn/cyanate ester composites were cured

by ramping the temperature to 113 °C and holding for 4 hrs, followed by a 1.5 hr hold at 135 °C. For the press mold cure process, the pressure was generally maintained at 1.38 MPa. Properties of the CNT yarn used and variables in the processing conditions used for each composite fabricated are provided in Table 1.

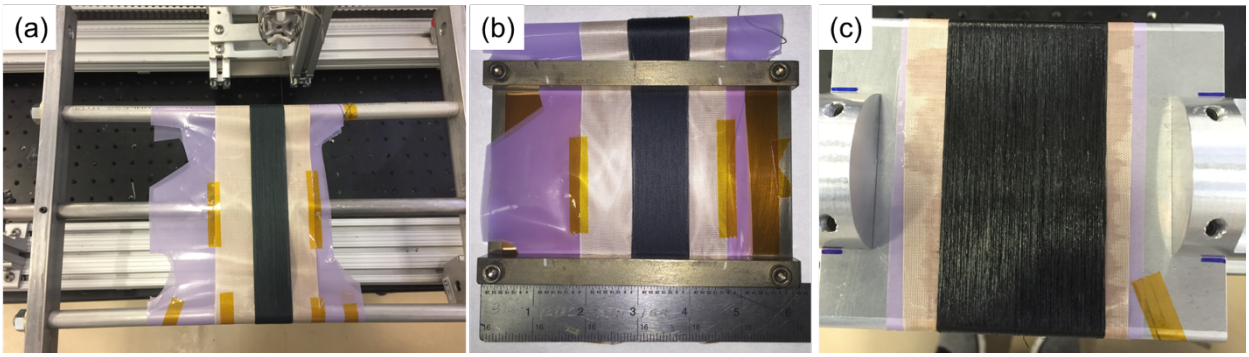

Figure 1. (a) Custom made stainless steel rod fixture (adjustable widths to 30.48 cm or 15.24 cm) and (b) cure mold with a pair of holding bars. (c) Unidirectional CNT yarn/API-60 composite (2-layers) wound on a solid aluminum fixture (10.16 cm × 15.24 cm) using a filament winder.

For the short beam shear test specimen, CNT yarns were directly wound onto a custom-made aluminum fixture (6.35 × 15.24 cm solid Al plate) by the wet winding process (70 wt.% solution of EPON™ in MEK) under 9.79 N winding tension. A stainless-steel guide was installed on each side of the Al fixture to constrain the CNT yarn winding width. The wound unidirectional CNT yarn/EPON™ 828 sample [6.35 (length) × 1.27 cm (width), 20 layers, 158 m of CNT yarn] was placed into the press, sandwiched between two Al bars, and cured under the same conditions described above. The resin content in the completed unidirectional CNT yarn/EPON™ 828 composite was 19 wt.% for the short beam shear test samples.

Table 1. Physical and mechanical properties of unidirectional CNT yarn/polymer composites.

Polymer composite	composite size (cm)	Winding tension (N)	Cure pressure (MPa)	# of yarn ply (total length)	CNT yarn strength [GPa/(g/cm^3)]	CNT yarn modulus [GPa/(g/cm^3)]	Tex (g/km)	Resin content (%)	Density (g/cm^3)	Thickness (μm)	Specific strength [GPa/(g/cm^3)]	Specific modulus [GPa/(g/cm^3)]
EPON^{TM} 828, 2 layers	15.24 x 2.54	2.49	1.38	4 (80 m)	1.68	55.5	28.712	14	0.816	356 ± 27	1.07 ± 0.04	51.5 ± 5.5
EPON^{TM} 828, 2 layers	15.24 x 2.54	9.79	1.38	4 (68 m)	1.55	57.1	25.234	14	0.891	239 ± 27	1.15 ± 0.13	52.8 ± 4.9
API-60, 1 layer	15.24 x 2.54	8.90	1.38	4 (118 m)	1.38	49.5	27.911	41	0.870	236 ± 2	0.84 ± 0.01	46.1 ± 7.5
API-60, 2 layers	10.16 x 5.08	9.79	1.38	4 (145 m)	1.64	56.3	23.911	17	0.972	418 ± 13	1.14 ± 0.08	77.6 ± 4.5
API-60, 2 layers	10.16 x 5.08	13.34	0.48 Autoclave	4 (145 m)	1.58	85.7	32.377	17	0.911	567 ± 31	1.09 ± 0.03	73.5 ± 6.5
API-60, 2 layers	30.48 x 2.54	Prepreg	1.38	4 (49 m)	1.30	73.7	27.827		0.805	297 ± 4	0.76 ± 0.04	46.0 ± 7.1
API-60, 3 layers	30.48 x 2.54	Prepreg	1.38	4 (67 m)	1.30	73.7	27.827		0.885	364 ± 9	0.75 ± 0.04	46.3 ± 3.9
Cyanate ester, 2 layers	10.16 x 2.54	13.34	10.34	4 (72 m)	1.63	96.3	26.888	19	1.143	383 ± 4	1.13 ± 0.03	72.3 ± 16.6
Cyanate ester, 2 layers	6.35 x 2.54	4.45	2.07	2 (90 m)	1.48	77.5	14.879	34	0.997	538 ± 11		
Cyanate ester, 1 layer	10.16 x 2.54	2.49	2.07	1 (20 m)	1.32	31.8	8.500	42	1.078	66 ± 3	0.70 ± 0.04	36.0 ± 0.8
EPON^{TM} 828, 20 layers	6.35 x 1.27	9.79	1.38	4 (158 m)	1.33	76.6	29.954	19		2794	Short beam shear test	Shear stress: 9.1 ± 0.4 MPa

Unidirectional CF (IM7, Hexcel)/API-60 composites were prepared from IM7/API-60 prepreg tape to enable property comparison with the unidirectional CNT yarn/polymer composites. Unsized IM7 CF tow (12K tow, tensile strength: 5.66 GPa, tensile modulus: 276 GPa, density: 1.78 g/cm^3, linear density: 446 g/km, tow cross sectional area: 0.25 mm^2) was passed through a resin bath (70 wt.% API-60 solution in MEK) to prepare an IM7/API-60 prepreg tape. The as-prepared IM7/API-60 prepreg tapes were placed into a press mold (7.62 × 15.24 cm) and cured as described above to form 2-ply unidirectional IM7/API-60 composites. The CF prepregger at NASA Langley Research Center has a capability of prepregging uni-tape from resin solution, films, and powders, as shown in Figure S1. Utilizing this prepregger, API-60 solution (70 wt.% API-60 in MEK) was used to coat both IM7 CFs and CNT yarns, which were used to fabricate conventional unidirectional tapes. Ten spools (~ 100 m each) of CNT yarn were fed through the resin bath side-by-side to make the unidirectional CNT yarn/API-60 prepreg tape (10 yarns, ~ 2 mm wide tape). The as-prepared unidirectional CNT yarn/API-60 prepreg tape was laid down and stacked on a press mold (2.54 × 30.48 cm) and then cured under the same cure conditions described above to form the unidirectional CNT yarn/API-60 composites. The properties of the resultant prepregs are presented in Table S1.

Measurements and Characterization. Room temperature tensile properties of unidirectional CNT yarn/polymer composites were measured using a MTS-858 test stand equipped with a laser extensometer and pneumatic grips. Sample thicknesses and densities are provided in Table 1. Composite thickness was determined using a profilometer-type instrument (Mitutoyo Corp., Model ID-S112PE). The nominal density was determined by measuring the length, width, thickness, and weight of the specimen. Tensile testing methods were based on ASTM standard D638 (standard test method for tensile properties of plastics) and D1708 (standard test method for tensile properties of plastics by use of microtensile specimens). The gauge length and cross head speed were approximately 20 mm (gap between two reflective tapes) and 0.5 mm/min, respectively. The tensile specimens were rectangular strips with a width of 5 mm and typical length of 10 cm, although lengths varied depending on the fixture used for winding (see Table 1 for composite sizes). A minimum of four specimens were tested to determine tensile strength and modulus. Specific tensile stress was calculated by dividing the measured failure force (N) by the linear density (g/km) of each specimen to eliminate errors associated with the measurement of sample thickness and specimen dimensions. Young's modulus was calculated from the slope between 10 and 30 % of ultimate tensile stress to eliminate the initial lag in stress-strain behavior.[19] Resin content was determined by measuring length and linear density of the CNT yarn used for each sample and the final composite weight.

Short beam shear specimens (nominally 2.79 mm thick, 5.08 mm wide, and 15.24 mm long, 5 samples) were cut using a high-speed precision diamond saw with a water/cutting fluid mixture as a coolant to ensure a clean cut. The short beam shear testing method was based on ASTM D2344 (standard test method for short beam strength of polymer matrix composite materials and their laminates), with the exception of a smaller specimen size. The support span

and diameters of the loading rod and support rods were 10.16 mm, 6.35 mm, and 3.18 mm, respectively.

Field emission-scanning electron microscopy (FE-SEM) images were acquired using a Hitachi S-5200 field-emission SEM system at an acceleration voltage of 30 keV using the secondary electron (SE) detector. Cross sectional SEM samples were prepared by a cooling cross sectional polisher (Jeol IB-19520CCP) using a 5 keV acceleration voltage under an argon plasma. The samples were cooled to -30 ^{o}C before polishing to prevent amorphous carbon build up on the polished surfaces. Transmission electron microscopy (TEM) images were acquired using a Jeol JEM-ARM200cF system at an acceleration voltage of 80 keV to minimize beam damage of the CNTs and polymer. Cross-sectional TEM samples were prepared using a focused ion beam (FIB, FEI Helios 600) system equipped with a precise positioning stage (OmniProbe^{TM}). The sample thickness was generally less than 30 nm and the CNTs were aligned at nearly 90 degrees to the sectioning direction. High resolution nondestructive evaluation of as-prepared unidirectional CNT yarn/polymer composites was conducted using a micro focus X-ray computed tomography (CT) system (Nikon Metrology) with a maximum resolution of 5 μm and magnification of up to 160×. A Perkin-Elmer 16-bit amorphous silicon digital detector with a 2000 × 2000 pixel array was used to collect radiographs at each rotation angle as the X-ray path intersected the sample (360 degrees in 0.11 degree increments). The three-dimensional reconstruction of the collected radiographs produced tomographic data that could be viewed along any plane in the sample volume.

Electrical conductivities of the unidirectional CNT yarn/polymer composites were determined using a measurement system consisting of custom built four-point electrodes, a Keithley 2400 current source, a Keithley 2000 digital multimeter, and software written in LabVIEW. The distance between the voltage probes was 1 cm. Eddy current conductivity measurements were acquired using a Jentek In-700-39 Meandering Winding Magnetometer

System with a FA150 bidirectional sensor operating at 10 MHz. The inductively coupled measurement technique utilizes a thin film driver/pickup coil pair and measures the complex trans-impedance of the coils. Data was acquired with the coil fixed as the sample was rotated 360 degrees beneath the coil. Impedance data was converted to lift-off (spacing between the coil and the sample under test) and conductivity of the part under testing through the use of a patented algorithm.[25] Calibration on conductivity samples of 0.02, 0.07, and 0.6 %IACS (1.2×10^4, 4.1×10^4, and 3.5×10^5 S/m, respectively) were used to bound the model. %IACS is the international annealed copper standard in which copper has a conductivity of 100 %IACS. A 4-ply unidirectional CF/polymer composite, fabricated with a standard epoxy resin [diglycidyl ether of bisphenol A (DGEBA)] and T700 CF (Toray), was used as a reference sample for Eddy current conductivity measurements. The unidirectional T700/DGEBA prepreg was prepared by hand layup and cured at 120 ^{o}C for 20 min using a half rigid mold and half vacuum bag.

Thermal conductivities of unidirectional CNT yarn/polymer composites at room temperature were measured by the transient plane source (TPS) method using a Hot Disk TPS 2500S (Thermtest Inc.). The Hot Disk sensor consists of an electrically conductive double spiral nickel pattern sandwiched between two thin sheets of electrically insulating Kapton® film. The sensor is used both as a heat source and as a dynamic temperature (resistance) sensor. A plane Hot Disk sensor (Type 5501, 6.403 mm radius) was placed between two pieces of the unidirectional CNT yarn/polymer composite with various stack angles or multiple layered stacks to measure the thermal conductivity and specific heat capacity by the Slab method. Thermal conductivities were measured at 200 mW of heating power and 2 sec of measurement time.

Results and Discussion

Morphological and mechanical properties of unidirectional CNT yarn/polymer composites. Two unidirectional CNT yarn/EPON™ 828 composites were fabricated by the wet winding process onto a 15.24 cm × 30.48 cm fixture (winding dimension: 15.24 cm × 2.54 cm, 2 layers). The composite processing conditions differed only in the applied winding tensions, which were 2.49 and 9.79 N. After curing under a pressure of 1.38 MPa, the composites (Figure 2a) were cut using a triple wavelength picosecond laser materials processing system (Photomachining Inc., Ekspla laser, 355 nm wavelength, 200 kHz frequency) at 75 % of beam attenuation with 10.16 cm/sec in mark speed and 50 repetitions to prepare the rectangular specimens (7.62 cm × 0.51 cm, Figure 2b). The resin content in both composites was 14 wt.%.

The thickness of the composite made under the higher winding tension (9.79 N, 239 μm) was less than that made under the lower winding tension (2.49 N, 356 μm) for the same length of CNT yarn used. This was mainly due to the greater consolidation of the CNT yarns under the higher winding tension. The physical result of the winding tension is visible in the x-ray CT image shown Figure 3, which illustrates the higher density and thinner cross-section that resulted from the greater compaction during composite processing. While the higher winding tension clearly results in greater composite consolidation, the x-ray CT images show that significant microstructural porosity still remains. This remaining internal fiber porosity results from the twisting together of 4 plies of CNT roving used to produce the yarns.[5] The roving is composed of large bundles of millimeter long CNTs, which are held together by van der Waals forces and impurities from the manufacturing process, including amorphous carbon and iron catalyst particles enclosed in graphitic shells. Individual plies within the 4-ply CNT yarn are physically entangled by a small amount of twisting applied during the manufacturing process. Alignment of the CNTs

and bundles in the roving during the manufacturing process is incomplete, which results in micro-sized voids throughout the yarn. The CNT yarns, with an average diameter of 200 μm, have irregular, elliptical shapes which further complicates the elimination of porosity in the final composites.

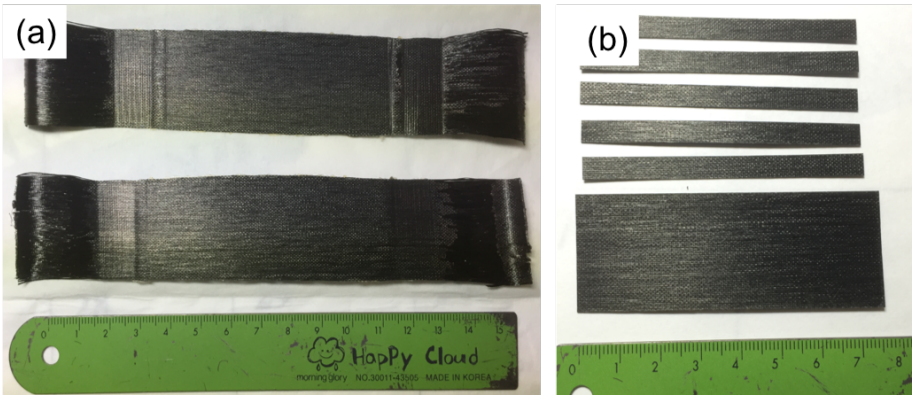

Figure 2. (a) As-prepared unidirectional CNT yarn/EPON™ 828 composite (2 layers). The composite was cured in a custom-made press mold equipped with a pair of corrugated bars to hold the wound CNT yarns under tension during cure. The CNT yarn between the bars only experienced high pressure (1.38 MPa) during the cure process. (b) As-prepared CNT yarn/EPON™ 828 composite was cut by a laser to create five rectangular tensile specimens (7.62 cm × 0.50 cm) and a coupon (7.62 cm × 2.54 cm) for thermal conductivity measurement.

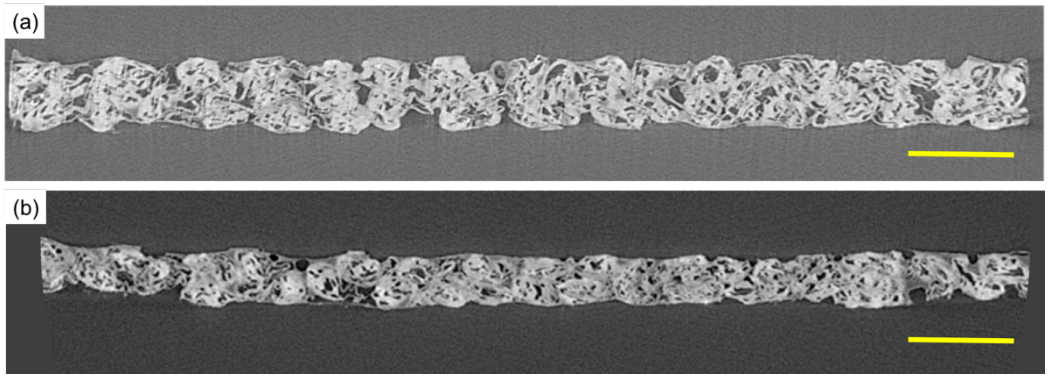

Figure 3. X-ray CT images of unidirectional CNT yarn/EPON™ 828 composites prepared using the wet winding method under (a) 2.49 and (b) 9.79 N winding tension, respectively. Scale bar is 500 μm.

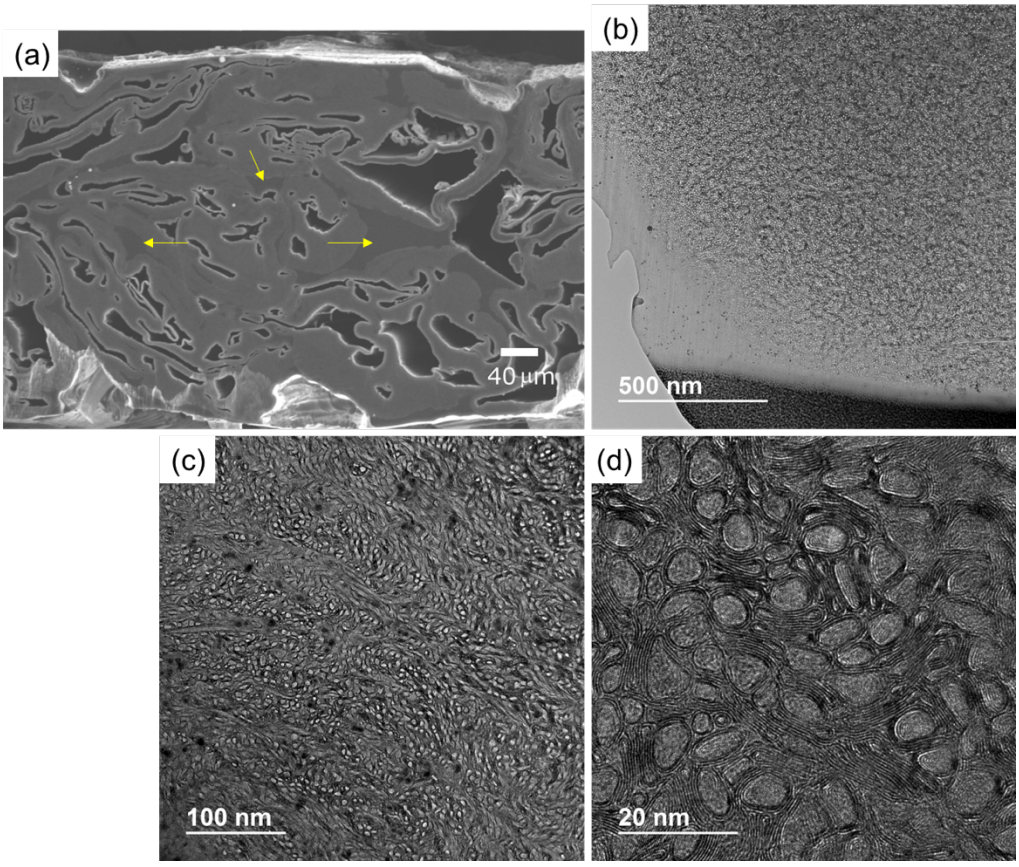

Figure 4. (a) FE-SEM and (b, c, and d) cross sectional TEM images of the unidirectional CNT yarn/EPON^{TM} 828 composite prepared at 2.49 N winding tension. TEM images were taken at several magnifications. Yellow arrows in (a) indicate resin rich regions.

Arrows in Figure 4a identify resin rich areas in the cross-sectional view of the composite. Figures 3 and 4a-b indicate that resin wet out inter-ply regions but failed to penetrate into the yarns during processing, although the ply surfaces are partially coated. Note that the resin content of this composite was 14 wt.%, which is relatively low compared to the 35 ~ 40 wt.% typically used in CF composites. Many voids, with sizes on the order of tens of microns and scattered both between and within the individual roving plies, are not filled with resin, indicating that they are closed voids which cannot be infiltrated by the resin. This is due to the presence of regions of densely packed CNTs in the yarn, as shown in cross sectional TEM images (Figures 4b, c, and d), which block

resin infiltration into the yarn. The CNTs in the yarn were generally double or triple walled, with average diameters of 7 ~ 8 nm, and were deformed into irregular oval and collapsed shapes. The large fraction of collapsed tubes produces higher packing densities than can be achieved with round CNTs, which accounts for the high-densities measured for the CNT yarns used in this work.[26]

Typical tensile stress-strain responses of the unidirectional CNT composites fabricated under the two different winding tensions are shown in Figure 5a. The two-layer unidirectional CNT yarn/EPON^{TM} 828 specimens, made under winding tensions of 2.49 and 9.79 N, failed catastrophically at various sites within the gauge regions during the tests (Figures 5b and c), which is similar to the failure behavior observed with unidirectional CF/polymer composites. Both tensile strength and modulus of the composites increased slightly with increased winding tension, as shown in Table 1. The specific strength of the composite wound at 2.49 N was 1.07 GPa/(g/cm^3), 64 % of the starting yarn value, while that of the composite wound at 9.79 N was 1.15 GPa/(g/cm^3), 74 % of the starting yarn value. The specific moduli and elongations at failure of the unidirectional CNT yarn composites were relatively unaffected by winding tensions, with both composites yielding values of ~ 52 GPa/(g/cm^3) and ~ 3 %. The composite specific moduli did not depend strongly on winding tensions, having values of 55.51 (2.49 N) and 57.14 GPa/(g/cm^3) (9.79 N), which are close to that of the starting yarn.

The results discussed to this point were obtained on composites prepared using the adjustable rod winding configuration. As previously noted, this method required the application of additional clamping tension when the sample was placed into the mold (Figures 1a and b) to retain yarn compaction and reduce interbundle voids. This complication, in combination with some degree of deformation of the fixture at high winding tensions, made it difficult to definitively determine the influence of winding tension in those composites. To mitigate these issues, a solid aluminum fixture (Figure 1c) was adopted, which allowed for a known tension to be maintained

during both the winding and curing steps. The results that follow were obtained with this improved fabrication fixture.

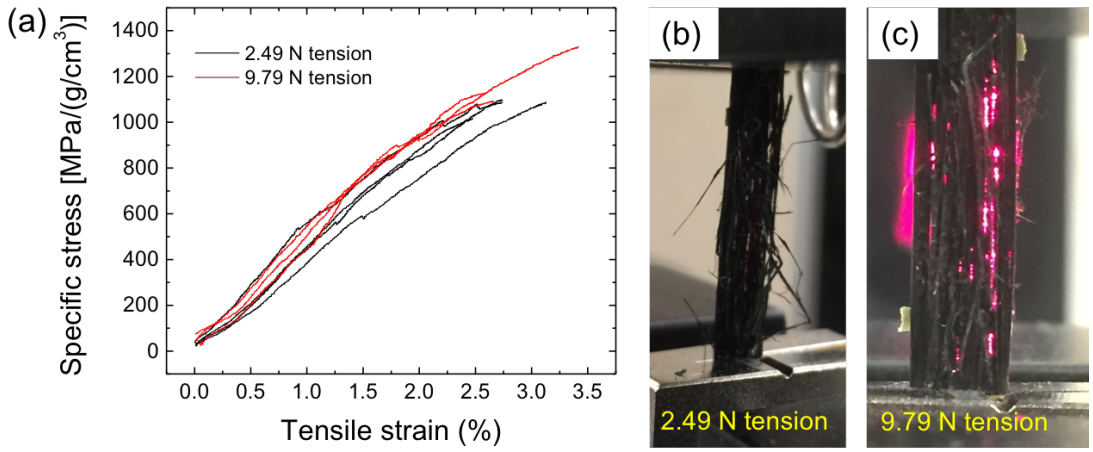

Figure 5. (a) Stress-strain curves of unidirectional CNT yarn/EPON^{TM} 828 composites prepared under winding tensions of 2.49 and 9.79 N. Digital photographs showed catastrophic failure of the unidirectional CNT yarn/EPON^{TM} 828 composites under a tensile load. The specimens were made under winding tensions of (b) 2.49 and (c) 9.79 N, respectively.

Figure 6 shows cross sectional x-ray CT images of a selection of these samples prepared with the Al plate fixture which illustrate the range of microstructures that resulted from these various processing conditions. For example, composites made under winding tensions of 9.79 N or less were very porous but had a relatively homogeneous distribution of CNTs, whether using 4-ply (Figure 6a) or 2-ply (Figure 6e) CNT yarns. For composites made at a higher winding tension of 13.34 N, it is easier to discern the individual yarns and to see the resin coating on their surfaces (Figures 6c and d). Micron size closed voids can be observed in the composites formed at both winding tensions, although it is difficult to distinguish individual yarns in the lower tension samples.

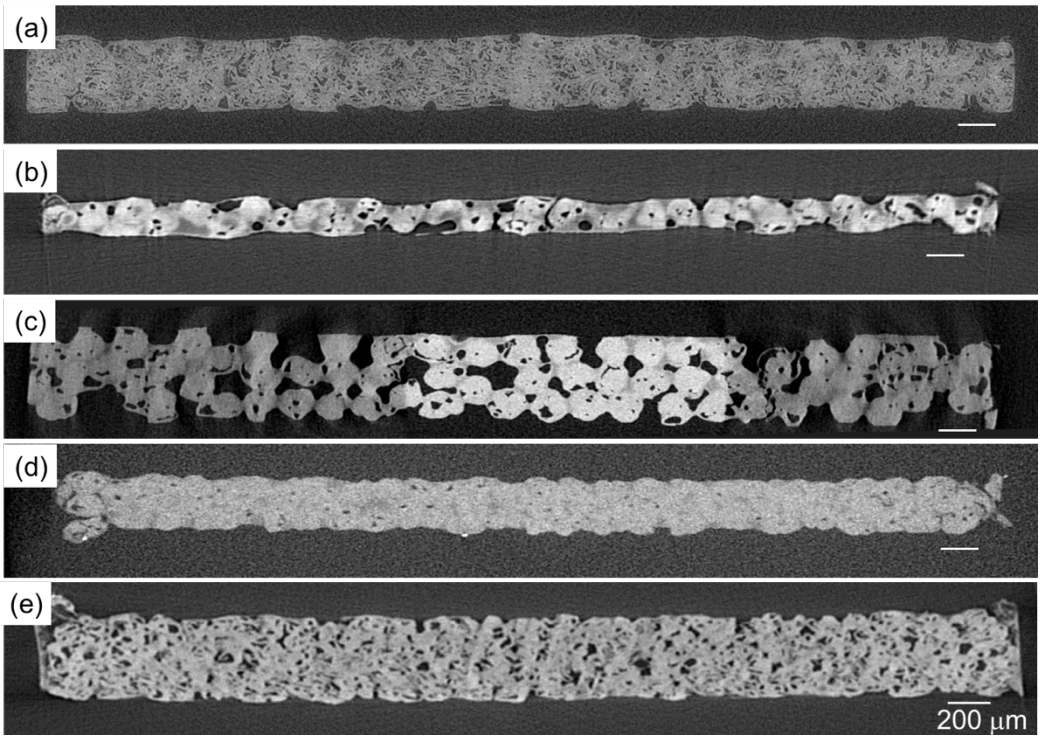

Figure 6. Cross sectional X-ray CT images of unidirectional CNT yarn/API-60 composites prepared under various processing conditions such as (a) 2 layers, 9.79 N winding tension, and 1.38 MPa cure pressure, (b) 2-layer lay-up of prepreg tape and 1.38 MPa cure pressure, and (c) 2 layers, 13.34 N winding tension, and autoclave cure. (d) Cross sectional X-ray CT image of the unidirectional CNT yarn/cyanate ester composite prepared with 2 layers of CNT yarn under 13.34 N winding tension and 10.34 MPa cure pressure. (e) Cross sectional X-ray CT image of the unidirectional CNT yarn/cyanate ester composite prepared with 2 layers of 2-ply CNT yarn under 4.45 N winding tension and 2.07 MPa cure pressure.

In general, the composites contain a distribution of opened (accessible) and closed (inaccessible) voids, which is most apparent in the autoclave cured composite shown in Figure 6c. The volume fractions of CNT, resin, and voids were computed as 55, 20, and 25 vol.%, respectively, using the ImageJ software package.[27] The computed volume fractions were based on the image contrast between the resin (lighter color around CNT yarn) and the CNT (darker and

rounded) using a user selected threshold adjustment. The calculated resin content of 20 vol.% was consistent with the experimentally determined resin content (17 wt.%) in the composite. The ability to quantify void volume fraction is useful in assessing the effectiveness of processing changes intended to reduce voids, such as winding tension and cure pressure. For example, Figure 6d shows a cross sectional x-ray CT image of unidirectional CNT yarn/cyanate ester composite prepared at a winding tension of 13.34 N and a press mold cure pressure of 10.34 MPa. The combination of higher winding tension and very high consolidation pressure yielded a composite with significantly lower void content (1.94 % by image analysis) and higher material density (1.143 g/cm^3), as calculated from the measured sample dimensions and weight. This calculated density is lower than a value of 1.526 ± 0.010 g/cm^3 measured using a pycnometer equipped with a custom-built sample container to accommodate rectangular specimens (Micromeritics, GA, USA, AccuPyc II 1340 Automatic Gas Pycnometer), which isolates the influence of open voids for the apparent density measurement.

Figure 7 shows a comparison of the specific strengths and moduli of various unidirectional CNT yarn/polymer composites. The corresponding values measured for the yarns used to fabricate the samples are indicated with star symbols in the figure. Note that the as-received yarn moduli progressively improved as the manufacturer refined their synthesis process during the course of this work, although the yarn strengths remained relatively constant. Despite the notable processing-induced differences in the composite morphologies observed in the CT-scans (Figure 6), the knock-downs in the specific strength, defined as the difference between the yarn and composite values, were all very close to 0.5 GPa/(g/cm^3). The one-layer CNT/API-60 composite, one of the two cases with a higher knock-down of 0.54 GPa/(g/cm^3), had a polymer matrix content of 41 wt.%. The fact that the other composite with a knock-down of 0.54 GPa/(g/cm^3), the two-layer CNT/API-60 composite, had a resin content similar to the other composites indicates that

resin content alone cannot fully explain the strength reduction. It is somewhat surprising that the high tension (13.34 N), high cure pressure (10.34 MPa) unidirectional CNT yarn/cyanate ester composite (fifth bar in Figure 7a) did not show improvement despite the significant void reduction and improved consolidation observed in the x-ray CT scan (Figure 6d). These results suggest that the specific tensile strength of unidirectional CNT yarn/polymer composites is much more dependent on yarn properties than any processing steps that may be taken in composite fabrication. This is consistent with CF composite behavior, although more detailed analysis is needed to better understand the tensile failure mechanism of these composites.

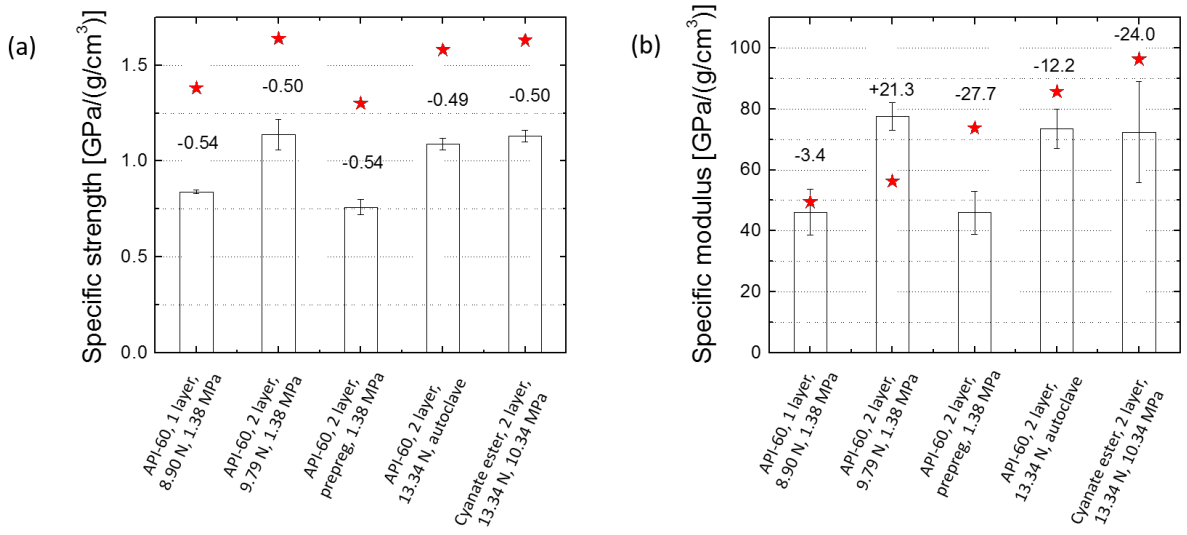

Figure 7. Comparison of (a) specific strength and (b) specific modulus of various unidirectional CNT yarn/polymer composites prepared under various winding tensions, cure pressures, consolidation methods, resin chemistries, and number of CNT yarn layers. The star symbols represent the corresponding values of the starting yarns. The numbers in the charts are the differences between the yarn and composite properties.

In contrast to the relative insensitivity of composite specific tensile strengths to processing variations, the specific moduli of the unidirectional CNT yarn/polymer composites show

significant differences. While no clear trends appear in the measured specific modulus data, a few particular cases warrant comment. First, the API-60 composite prepared from the prepreg shows a notably large knock-down as indicated in Figure 7. This is likely due to an elevated resin content and separation between the matrix and CNT constituents, as noted above in the discussion of specific strength and shown in Figure 6b. Second, the high tension, high pressure cyanate ester composite again performed much more poorly than was expected in light of its dense, consolidated microstructure. Finally, the specific modulus of the unidirectional CNT yarn/API-60 composite with 2-layers of CNT yarn (winding tension of 9.79 N and cure pressure of 1.38 MPa) significantly improved relative to the modulus of the starting yarn. Further work will be needed to understand this unexpected result.

Given the broad and commercially important use of prepregging in conventional CF composite fabrication, it was of interest to better understand the mechanical properties observed for the composite prepared from prepregged CNT yarn and API-60. To do so, additional cross-sectional FE-SEM images of the prepregged composite were taken and are shown in Figure 8. Figure 8a reveals the uneven thickness in the composite and the nonuniform spacing between the CNT yarns, which likely resulted from the limited processing resolution of the CF prepreg machine. The resin from the two CNT yarn prepreg layers appears to have consolidated during the press mold process, despite the relatively lower cure pressure (1.38 MPa), resulting in large continuous resin rich areas. Consequently, the prepregged composite had a relatively lower thickness (297 μm) and lower nominal density (0.805 g/cm^3) compared to those from the winding process (9.79 N winding tension) composite (418 μm and 0.972 g/cm^3, respectively). It is also of interest to note that a crack develops within a CNT yarn rather than at the yarn/matrix interface or in the outermost portion of the yarn, as shown in Figure 8b. This implies that the resin/yarn interfacial adhesion is reasonably strong and that the resin penetrates some distance into the outer

layers of the yarn. The fact that the crack develops in the inner portion of the yarn indicates that the resin has not fully penetrated the yarn, possibly due to high CNT packing densities in the inner portion. Figure 8c, which shows unfilled porosity within the CNT rich zone, supports this inference.

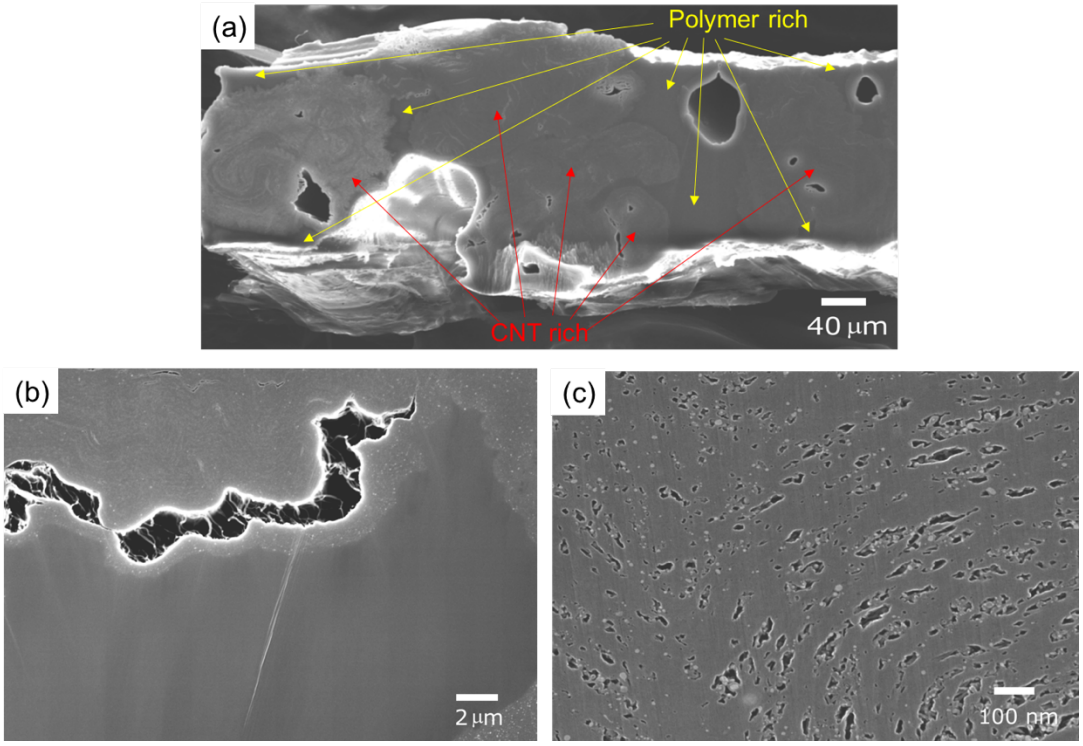

Figure 8. Cross sectional FE-SEM images of unidirectional CNT/API-60 composite prepared from prepreg tape. Images were taken at magnifications of (a) 200, (b) 5K and (c) 100K.

By now it is clear that completely infiltrating the CNT yarn during the composite fabrication process is challenging due to closed voids, with dimensions of tens of nanometers, that remain after high tension winding and high-pressure composite processing. An alternate approach to avoid both inter- and intra-yarn porosity is the use of much thinner CNT yarns. To test this hypothesis, 2-ply and 1-ply yarns were utilized to fabricate double layered and single layered unidirectional CNT yarn/cyanate ester composites, respectively. Relative to the 4-ply CNT yarns, lower winding tensions were required to accommodate the lower breaking strengths of the thinner

yarns and, due to the larger total yarn surface area, larger quantities of resin were retained in the composites (34 wt.% for 2-ply vs. 17 wt.% for 4-ply) despite the use of higher cure pressure (2.07 MPa) during the press molding step. The composites resulted in slightly higher densities (0.997 g/cm^3 for 2-ply vs. 0.972 g/cm^3 for 4-ply) and thicker samples (538 μm for 2-ply vs. 418 μm for 4-ply). The stress-strain curves for the 1-ply CNT yarn composites, shown in Figure 9, exhibit a saw-tooth failure process between 2 and 4 % tensile strain, indicating a series of individual yarn failures at different times and locations. Although there is a significant knock-down in the specific strength in the composite (47 % relative to an individual 1-ply yarn), the specific modulus increased from 31.8 (pristine single ply CNT yarn) to 36.0 GPa/(g/cm^3). This was unexpected due to the relatively high resin content (42 wt.%) in the composite and indicates a synergistic interaction between the yarn and matrix that increased composite stiffness. Unfortunately, the 2-ply yarn composite could not be tested mechanically under a tensile load due to slippage at the grips.

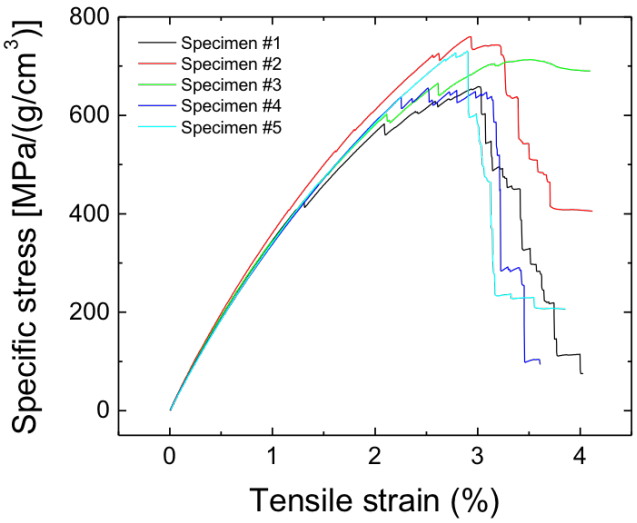

Figure 9. Stress-strain curves of the 1-ply unidirectional CNT yarn/cyanate ester composite.

To allow an assessment of the results obtained for the CNT yarn composites relative to a state-of-the-art composite, aerospace grade CF composite was fabricated and tested. Figure 10a shows the stress-strain curves of unidirectional IM7/API-60 composites (2-ply, 254 μm thickness). Catastrophic failure of the composite, shown in Figure 10b, was observed at a strain of around 2.6 %. The specific strength and specific modulus of the unidirectional IM7/API-60 composite were 1469 ± 87 MPa/(g/cm^3) and 60 ± 4 GPa/(g/cm^3), respectively, which are 45 % and 39 % as large as the corresponding values measured for an individual IM7 CF. A FE-SEM image of the failure site of the unidirectional IM7/API-60 composite is shown in Figure 10c. This image shows that the CFs were well wetted out with no visible voids and no fiber pulled-out in the region examined. Taken together, these observations suggest good interfacial adhesion between the CFs and the matrix and that the composite failed by brittle fracture in multiple locations (Figure 10b). This is in contrast to the unidirectional CNT yarn/polymer composites that exhibited both significant porosity and resin rich areas, both of which had a deleterious effect on composite properties. Despite these problems, the CNT composites still retained a higher percentage of the native yarn properties than did the CF composites. The property retention allows for the possibility that continuing improvements in yarn synthesis techniques and CNT yarn composite fabrication methods could result in CNT composite properties that exceed what is possible with CF composites.

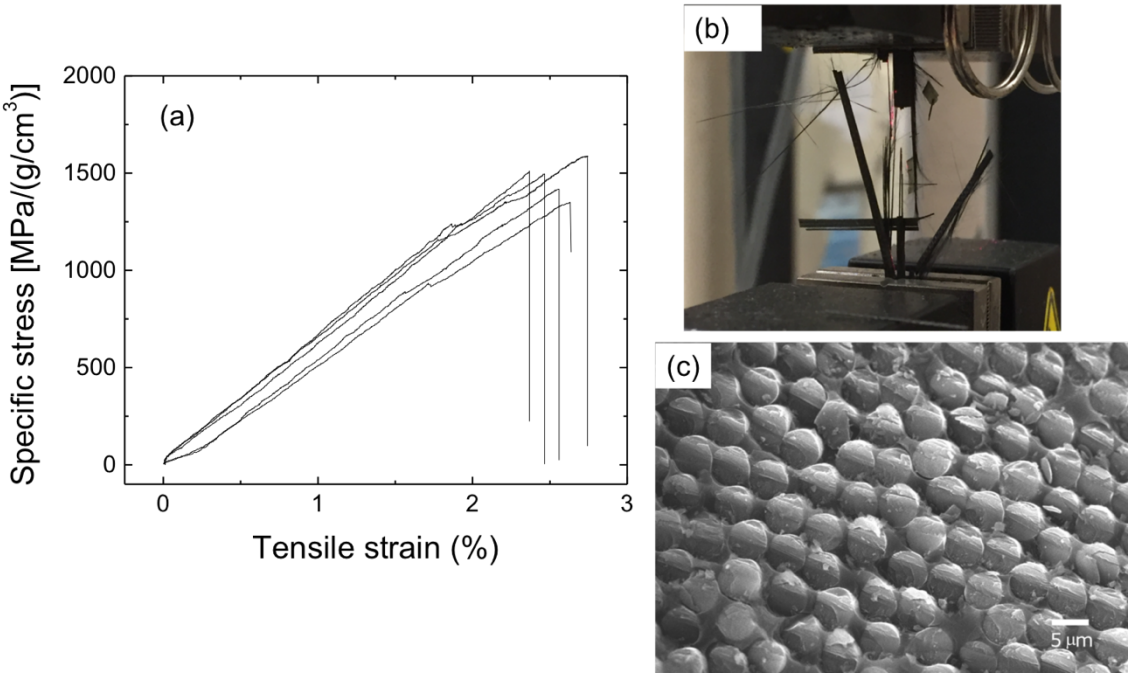

Figure 10. (a) Stress-strain curves and (b) digital photograph at the moment of failure of unidirectional IM7/API-60 composite. (c) Cross-sectional FE-SEM image of the failure site on the tested unidirectional IM7/API-60 composite.

Finally, Figure 11 shows the load vs. extension curves of unidirectional CNT yarn/EPON^{TM} 828 composites during short beam shear testing. The 2.8 mm thick unidirectional CNT yarn/EPON^{TM} 828 composite contained 20 layers of CNT yarns, a resin content of 19 wt.%, and was wound under a winding tension of 9.79 N. The specimen failed by an inelastic deformation mode during the test, due primarily to insufficient resin content in the composite and porous micro-structure. While the results of the test are not strictly valid because the failure mode differed from that required by the ASTM standard, we note that the measured shear stress, 9.1 ± 0.4 MPa, is an order of magnitude lower than the literature value for unidirectional IM7(12k tow)/8552 composite (~137 MPa).[28] More experiments will be needed to clarify the failure mode of the CNT composite to find an optimum resin content for shear strength and CNT yarn/resin interface properties.

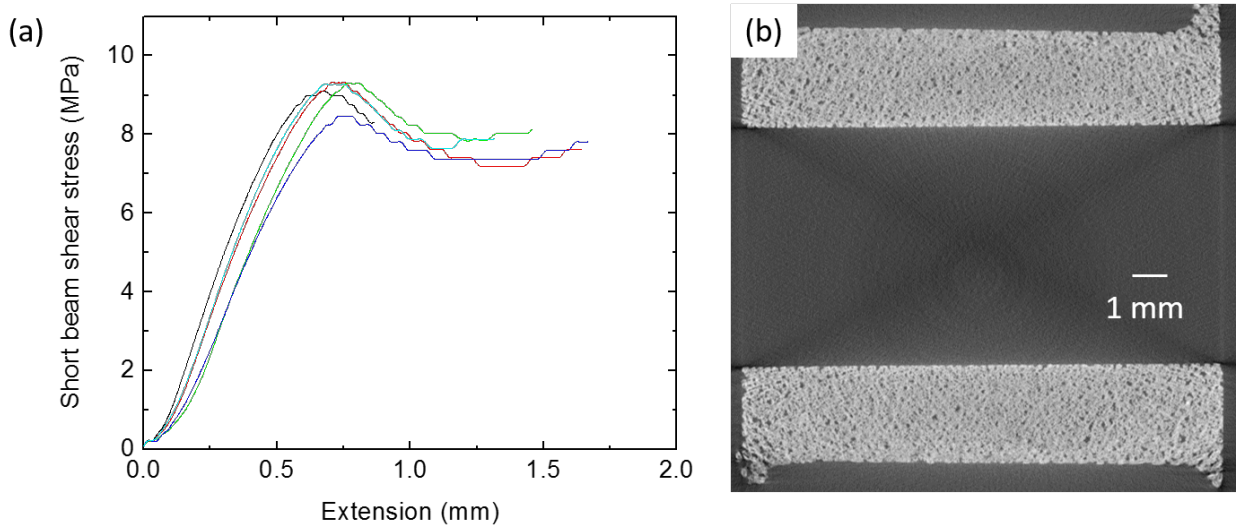

Figure 11. (a) Load-displacement curves and (b) x-ray CT image of the unidirectional CNT yarn/EPON^{TM} 828 composite fabricated for short beam shear test specimens.

Electrical properties of unidirectional CNT yarn/polymer composites. Electrical conductivities of the unidirectional CNT yarn/polymer composites were measured using a custom-built four-point electrodes measurement system. Current-voltage (IV) curves were generated by four test strips spanning two pairs of electrodes with a 1 cm gap between the innermost pair. Current was swept from 0 to 1 A and back to 0 A through the outer electrode pair with the voltage measured across the inner pair. Figure 12a shows typical IV curves for the unidirectional CNT yarn/EPON^{TM} 828 composites prepared at 2.49 and 9.79 N of winding tension. Figure 12b shows the electrical conductivity of both composites and the pristine CNT yarn. The composites had significantly lower conductivity than the yarn due to the added resin, which does not contribute to current carrying capacity. For this limited sample set, winding tension did not appear to affect the measured conductivity significantly, with the values being equivalent within experimental error. The higher winding tension did lead to less data scatter, suggesting reduced variability between

samples. Overall, electrical conductivity of unidirectional CNT yarn/polymer composites was in the range 1000 to 12000 S/cm, which is significantly higher than that from unidirectional IM7/8552 composites (19.9 S/cm).[29]

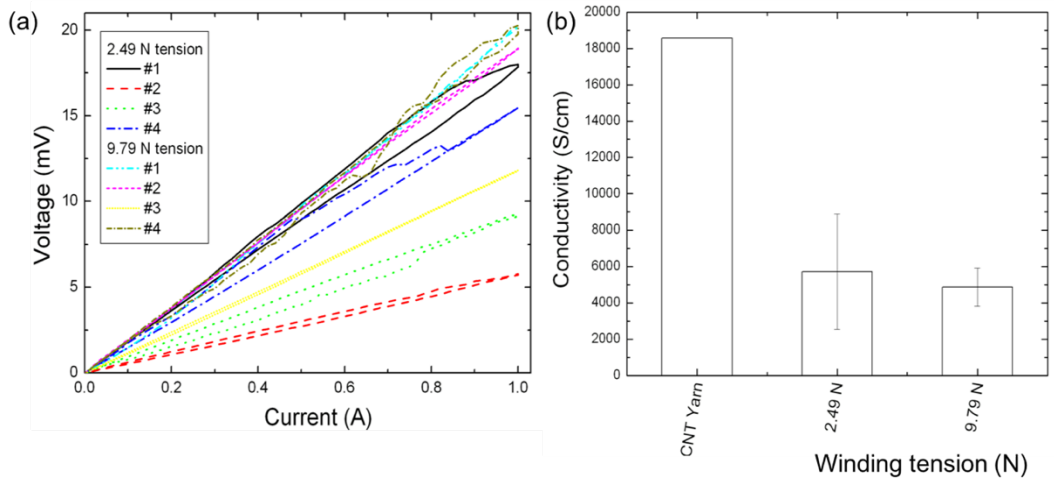

Figure 12. (a) Typical current-voltage curves and (b) DC electrical conductivities of unidirectional CNT yarn/EPON™ 828 composites prepared under 2.49 and 9.79 N of winding tension.

Eddy current data was acquired by placing the sensor on top of a 2-layer unidirectional CNT yarn/API-60 composite or 4-ply unidirectional CF composite and acquiring impedance data as the composite was rotated by a stepper motor. The inductive measurement is affected by sample thickness because the depth of penetration of the induced currents decays exponentially with depth into the sample. At a high enough conductivity and frequency, the vast majority of the electromagnetic field is contained within the sample, and further increases in sample thickness make little or no difference in the measured conductivity. For thin or low conductivity samples, however, a significant portion of the field will penetrate through the sample. In these cases, changes in thickness will have a major effect. The depth of penetration of the field into the sample can be estimated from a skin depth calculation. Using a conductivity of 0.12 %IACS and a frequency of 10 MHz, the skin depth was calculated to be 603 μm. This would be the depth that

the field decays to 1/3 of its value at the surface. The measured conductivity can be bounded by using the uncorrected values given in Figure 13 as a minimum conductivity and the thickness weighted conductivity as the upper bound. A simple weighting of the eddy current conductivity measurement with sample thickness as

$$\sigma_{measured} = \sigma_{actual} * \frac{Sample\ thickness\ (skindepths)}{3}$$

(for sample thickness less than or equal to the measurement depth of 3 skin depths) can be used as the thickness weighted upper bound. In this case, the upper bound for the conductivity of the unidirectional CF composite would be 0.007 %IACS × 3/(0.841 mm/2.5 mm) = 0.062 %IACS. Likewise, the upper bound for the unidirectional CNT yarn/API-60 composite conductivity is given by 0.12 × 3/(0.419 mm/0.603 mm) = 0.52 %IACS. The penetration depths of the unidirectional CF composite and the unidirectional CNT yarn/API-60 composite were calculated to be 2.5 and 0.603 mm, respectively, while the sample thicknesses were measured to be 0.841 and 0.419 mm, respectively. Both samples show clear conductivity peaks along the fiber direction of the uniaxial parts.

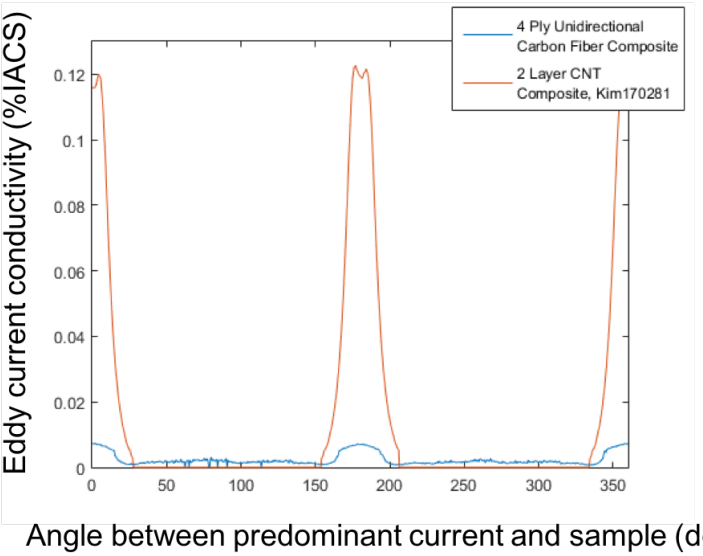

Figure 13. Eddy current conductivities of unidirectional CNT yarn/API-60 and 4-ply unidirectional carbon fiber composites.

Thermal properties of unidirectional CNT yarn/polymer composites. Thermal conductivities of the unidirectional CNT yarn/EPON^{TM} 828 composites fabricated under 2.49 and 9.79 N of winding tension, stacked and aligned in various sequences, and measured using a Thermtest TPS 2500S system, are shown in Table 2. The thermal conductivities of the unidirectional CNT yarn/EPON^{TM} 828 composite fabricated at 9.79 N of winding tension are 32.07 and 45.33 W/m·K with 0^o|||0^o and 0^o|||90^o stacks, respectively. These values were larger than those for the composite fabricated at 2.49 N winding tension (21.98 and 32.86 W/m·K with 0^o|||0^o and 0^o|||90^o stacks, respectively). This is due to the consolidation of the CNT yarns under the higher winding tension. The thermal conductivity of the 0^o|||90^o stack of both composites, fabricated at 2.49 and 9.79 N of winding tension, was 35.79 W/m·K, which is in between the values measured with each composite. Thermal conductivities of the double stacked samples decreased due to increasing number of interfaces between the samples at $0^o/90^o$, $0^o/0^o$, and $90^o/90^o$ stacks. However, the thermal conductivities of unidirectional CNT yarn/polymer composites with various stack angles are higher than that from unidirectional IM7/8552 composites (5.5 W/m·K at R.T.) and their hybrid composites with CNT sheets (<10 W/m·K at various temperatures).[30] Measured specific heat capacities of the composites with various stacks ranged between 1.37 and 3.30 J/g·K. Note that the specific heat capacity, as determined by differential scanning calorimetry (DSC, Netzsch DSC 204 F1), was 1.75 J/g·K, in good agreement with the values measured using the TPS.

Table 2. Thermal Conductivities of the unidirectional CNT Yarn/EPON^{TM} 828 Composites.

Sample	Stack degree	Thermal conductivity (W/m·K)	Specific Heat capacity (J/g·K)
9.79 N tension	0^o ||| 0^o	32.07	2.19
	0^o ||| 90^o	45.33	1.97
2.49 N tension	0^o ||| 0^o	21.98	1.45
	0^o ||| 90^o	32.86	1.37
9.79 N ||| 2.49 N	0^o ||| 90^o	35.79	2.13
9.79 N ||| 2.49 N	$0^o/0^o$ ||| $90^o/90^o$	16.67	2.98
9.79 N ||| 2.49 N	$0^o/90^o$ ||| $90^o/0^o$	21.24	2.40
9.79 N ||| 2.49 N	$0^o/90^o$ ||| $0^o/90^o$	21.70	3.30

Conclusions

Unidirectional CNT yarn/polymer composites were fabricated under varying processing conditions including number of CNT yarn layers, CNT yarn/resin ratio, resin chemistry, tension applied during CNT yarn winding, and consolidation method. The effects of these processing variations were assessed by investigating micro-structural morphologies, mechanical performance under tensile and short beam shear loads, and electrical and thermal conductivities of unidirectional CNT yarn/polymer composites. The micro-structural morphology and void content in the composites were found to improve when using higher tensions during the winding process and higher cure pressures during the press molding step. Surprisingly, the specific tensile strength of the composites was not significantly affected by any of the fabrication parameters tested, even though the high tension winding and high pressure cure processes were found to improve the morphology of the CNT yarn/polymer composites by reducing porosity. These results indicate that adjusting composite fabrication processes with current CNT yarn formats will not be enough to overcome limitations in the yarn and resin starting materials. Continuing improvement in high strength CNT yarn manufacturing methods and additional optimization of resin chemistry to enable better CNT yarn/matrix adhesion are needed before composite fabrication processes can be

optimized. If achieved, the improved mechanical, electrical and thermal conductivities, of unidirectional CNT yarn/polymer composites could constitute a promising material for numerous multifunctional structural applications in aerospace vehicles.

References

1. Subramaniam C, Yamada T, Kobashi K, Sekiguchi A, Futaba DN, Yumura M, Hata K. One hundred fold increase in current carrying capacity in a carbon nanotube-copper composite. Nat Commun 2013; 4: 2202
2. Mirri F, Orloff N, Forster AM, Ashkar R, Headrick RJ, Bengio EA, Long CJ, Choi A, Luo Y, Hight Walker AR, Butler P, Migler KB, Pasquali M. Lightweight, flexible, high-performance carbon nanotube cables made by scalable flow coating. ACS Appl Mater & Interfaces 2016; 8: 4903-4910.
3. Chaudhary A, Kumari S, Kumar R, Teotia S, Singh BP, Singh AP, Dhawan SK, Dhakate SR. Lightweight and easily foldable MCMB-MWCNTs composite paper with exceptional electromagnetic interference shielding. ACS Appl Mater & Interfaces 2016; 8: 10600-10608.
4. Baur J, Solverman E. Challenges and opportunities in multifunctional nanocomposite structures for aerospace applications. MRS Bulletin 2007; 32: 328-334.
5. Kim JW, Sauti G, Cano RJ, Wincheski RA, Ratcliffe JG, Czabaj M, Gardner NW, Siochi EJ. Assessment of carbon nanotube yarns as reinforcement for composite overwrapped pressure vessels. Comps Part A 2016; 84: 256-265.
6. Treacy MMJ, Ebbesen TW, Gibson JM. Exceptionally high Young's modulus observed for individual carbon nanotubes. Nature 1996; 381: 678-680.

7. Wong EW, Sheenhan PE, Lieber CM. Nanobeam mechanics: elasticity, strength, and toughness of nanorods and nanotubes. Science 1997; 277: 1971-1975.
8. Yu MF, Lourie O, Dyer MJ, Moloni K, Kelly TF, Ruoff RS. Strength and breaking mechanism of multiwalled carbon nanotubes under tensile load. Science 2000; 287: 637-640.
9. Zhu Y, Espinosa HD. An electromechanical material testing system for in situ electron microscopy and applications. Proc Natl Acad Sci USA 2005; 102: 14503-14508.
10. Xie XL, Mai YW, Zhu XP. Dispersion and alignment of carbon nanotubes in polymer matrix: A review. Mater Sci Eng R 2005; 49: 89-112.
11. Moniruzzaman M, Winey KI. Polymer nanocomposites containing carbon nanotubes. Macromolecules 2006; 39: 5194-5205.
12. Coleman JN, Khan U, Blau WJ, Gun'ko YK. Small but strong: A review of the mechanical properties of carbon nanotube-polymer composites. Carbon 2006; 44: 1624-1652.
13. Spitalsky Z, Tasis D, Papagelis K, Galiotis C. Carbon nanotube-polymer composites: Chemistry, processing, mechanical and electrical properties. Prog Polym Sci 2010; 35: 357-401.
14. Byrne MT, Gun'ko YK. Recent advances in research on carbon nanotube-polymer composites. Adv Mater 2010; 22: 1672-1688.
15. Mora RJ, Vilatela JJ, Windle AH. Properties of composites of carbon nanotube fibers. Compos Sci Technol 2009; 69: 1558-1563.
16. Cheng Q, Bao J, Park JG, Liang Z, Zhang C. Wang B. High mechanical performance composite conductor: Multi-walled carbon nanotube sheet/bismaleimide nanocomposites. Adv Funct Mater 2009; 19: 3219-3225.

17. Cheng Q, Wang B, Zhang C, Liang Z. Functionalized carbon-nanotube sheet/biamaleimide nanocomposites: Mechanical and electrical performance beyond carbon-fiber composites. Small 2010; 6: 763-767.
18. Kim JW, Siochi EJ, Carpena-Núñez J, Wise KE, Connell JW, Lin Y, Wincheski RA. Polyaniline/carbon nanotube sheet nanocomposites: Fabrication and characterization. ACS Appl Mater Interfaces 2013; 5: 8597-8606.
19. Kim JW, Sauti G, Siochi EJ, Smith JG, Wincheski RA, Cano RJ, Connell JW, Wise KE. Toward high performance thermoset/carbon nanotube sheet nanocomposites via resistive heating assisted infiltration and cure. ACS Appl Mater Interfaces 2014; 6: 18832-18843.
20. Han Y, Zhang X, Yu X, Zhao J, Li S, Liu F, Gao P, Zhang Y, Zhao T, Li Q. Bio-inspired aggregation control of carbon nanotubes for ultra-strong composites. Sci Rep 2015; 5: 11533.
21. Xu W, Chen Y, Zhan H, Wang JN. High-strength carbon nanotube film from improving alignment and densification. Nano Lett 2016; 16: 946-952.
22. Li Z, Liang Z. Optimization of buckypaper-enhanced multifunctional thermoplastic composites. Sci Rep 2017; 7: 42423.
23. Park OK, Choi H, Jeong H, Jung Y, Yu J, Lee JK, Hwang JY, Kim SM, Jeong Y, Park CR, Endo M, Ku BC. High-modulus and strength carbon nanotube fibers using molecular cross-linking. Carbon 2017; 118: 413-421.
24. Shang Y, Wang Y, Li S, Hua C, Zou M, Cao A. High-strength carbon nanotube fibers by twist-induced self-strengthening. Carbon 2017; 119: 47-55.
25. Goldfine N. J., Schlicker D. E., Washabaugh A. P. Absolute Property Measurement with Air Calibration. US Patent RE39,206, 2006; July 25.

26. Downes RD, Hao A, Park JG, Su YF, Liang R, Jensen BD, Siochi EJ, Wise KE. Geometrically constrained self-assembly and crystal packing of flattened and aligned carbon nanotubes. Carbon 2015; 93: 953-966.
27. Rasband WS, ImageJ. U.S. National Institutes of Health, Bethesda, Maryland, USA, Retrieved June 25, 2018 from https://imagej.nih.gov/ij/, 1997-2016.
28. Hexcel Datasheet for Typical HexPly® 8552 Epoxy Resin Composite Properties. Retrieved June 25, 2018 from http://www.hexcel.com/Products/Resources/1664/hextow-laminate-properties-in-hexply-8552.
29. Grimsley BW, Cano RJ, Kinney MC, Pressley J, Czabaj MW, Siochi EJ, Sauti G, Kim J-W. Characterization of hybrid CNT polymer matrix composites. SAMPE Proceedings 2015; A-6476.
30. Kang JH, Cano RJ, Ratcliffe JG, Luong H, Grimsley BW, Siochi EJ. Multifunctional hybrid carbon nanotube/carbon fiber polymer composites. SAMPE Proceedings 2016; LB15-0246.

Supporting Information:

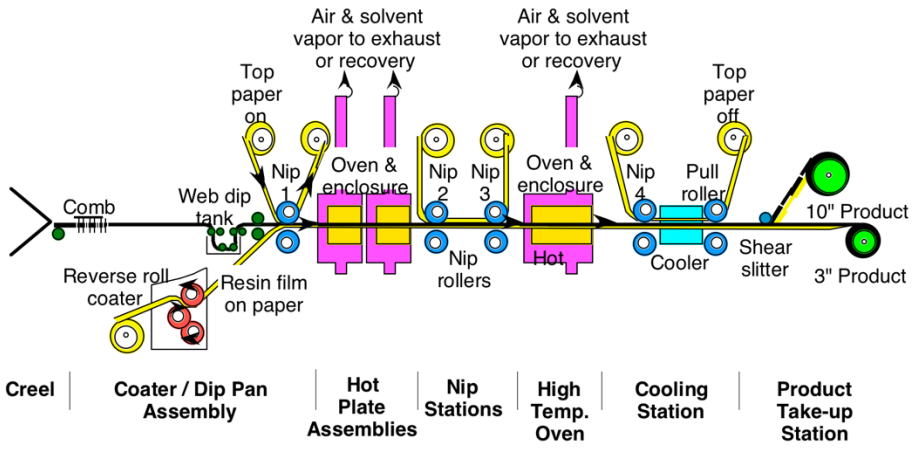

Figure S1. Schematic of LaRC multipurpose prepreg machine.[S1]

Table S1. API-60 epoxy unidirectional prepreg characteristics.

Fiber/ Sizing	Fiber Areal Weight, g/m^2	Volatiles, wt% (wet)	Resin, wt% (dry)	Length, m	Width, cm
IM7/ Unsized	131-140	4.3-4.9	35-38	23	11
CNT Yarn/ Unsized	N/A	7.1-10.5	62-69	8	0.32
CNT Yarn/ Unsized	N/A	5.4-7.2	51-56	11	0.32

S1. Cano R J, Johnston N J, Marchello J. 40th SAMPE Symposium and Exhibition, Anaheim, CA, 1995: May.

REPORT DOCUMENTATION PAGE

Form Approved
OMB No. 0704-0188

1. REPORT DATE *(DD-MM-YYYY)*
1-07-2018

2. REPORT TYPE
Technical Memorandum

3. DATES COVERED *(From - To)*

4. TITLE AND SUBTITLE

Unidirectional Carbon Nanotube Yarn/Polymer Composites

5a. CONTRACT NUMBER

5b. GRANT NUMBER

5c. PROGRAM ELEMENT NUMBER

6. AUTHOR(S)

Kim, Jae-Woo; Sauti, Godfrey; Cano, Roberto J.; Jensen, Benjamin D.; Smith, Joseph G.; Wise, Kristopher; Siochi, Emilie J.; Wincheski, Russell A.

5d. PROJECT NUMBER

5e. TASK NUMBER

5f. WORK UNIT NUMBER
432938.02.07.03

7. PERFORMING ORGANIZATION NAME(S) AND ADDRESS(ES)

NASA Langley Research Center
Hampton, VA 23681-2199

8. PERFORMING ORGANIZATION REPORT NUMBER
L-20949

9. SPONSORING/MONITORING AGENCY NAME(S) AND ADDRESS(ES)

National Aeronautics and Space Administration
Washington, DC 20546-0001

10. SPONSOR/MONITOR'S ACRONYM(S)
NASA

11. SPONSOR/MONITOR'S REPORT NUMBER(S)
NASA-TM-2018-220081

12. DISTRIBUTION/AVAILABILITY STATEMENT

Unclassified
Subject Category 24
Availability: NASA STI Program (757) 864-9658

13. SUPPLEMENTARY NOTES

14. ABSTRACT Carbon nanotubes (CNTs) are one-dimensional nanomaterials with outstanding electrical and thermal conductivities and mechanical properties at the nanoscale. With these superior physical properties, CNTs are very attractive materials for future light weight structural aerospace applications. Recent manufacturing advances have led to the availability of bulk formats of CNTs such as yarns, tapes, and sheets in commercial quantities, thus enabling the development of macro-scale composite processing methods for aerospace applications. The fabrication of unidirectional CNT yarn/polymer composites and the effect of processing parameters such as resin type, number of CNT yarn layers, CNT yarn/resin ratio, consolidation method, and tension applied during CNT yarn winding on the mechanical properties of unidirectional CNT yarn composites are reported herein. Structural morphologies, electrical and thermal conductivities, and mechanical performance of unidirectional CNT yarn/polymer composites under tensile and short beam shear loads are presented and discussed. The application of higher tension during the winding process and elevated cure pressure during the press molding step afforded a compact structural morphology and reduced void content in the composite.

15. SUBJECT TERMS

Carbon nanotube; Composite; Mechanical property

16. SECURITY CLASSIFICATION OF:			17. LIMITATION OF ABSTRACT	18. NUMBER OF PAGES	19a. NAME OF RESPONSIBLE PERSON
a. REPORT	b. ABSTRACT	c. THIS PAGE			STI Help Desk (email: help@sti.nasa.gov)
U	U	U	UU	37	19b. TELEPHONE NUMBER *(Include area code)* (757) 864-9658